

## Interface States at Ultrathin Chemical Oxide/Silicon Interfaces Obtained from Measurements of XPS Spectra under Biases

Hikaru Kobayashi, Yoshiyuki Yamashita, Kenji Namba, Yoshihiro Nakato, and Yasuhiro Nishioka\*

*Department of Chemistry, Faculty of Engineering Science, and Research Center for Photoenergetics of Organic Materials, Osaka University, Toyonaka, Osaka 560, Japan*

*\*Tsukuba Research and Development Center, Texas Instruments Japan, 17 Miyukigaoka, Tsukuba, Ibaraki, 305 Japan*

The energy distribution of interface states in the Si band-gap for MOS devices with an ultrathin chemical oxide layer has been obtained from measurements of XPS spectra under biases. The energy distribution has peaked structure. The peak near the midgap is attributed to isolated Si dangling bonds whereas the peaks below and above the midgap are attributed, respectively, to the Si dangling bonds interacting weakly with Si and oxygen atoms in the silicon oxide layer.

### §1. Introduction

Interface states in the Si band-gap seriously affect the electrical characteristics of metal-oxide-semiconductor (MOS) devices. However, it is very difficult to obtain the energy distribution of interface states for MOS devices with an ultrathin oxide layer from the conventional measurements of electrical characteristics such as capacitance-voltage<sup>1, 2)</sup> and conductance-voltage<sup>3)</sup> characteristics, because a tunneling current flows through the thin oxide layer. In the present study, the energy distribution of interface states for MOS devices with an ultrathin chemical oxide layer is obtained from a new method developed by us, i.e., measurements of XPS spectra under biases.<sup>4-7)</sup>

Various kinds of chemical oxide layers are formed during the wafer cleaning process. It is very likely that, for MOS devices with an ultrathin oxide layer, the chemical oxide layer present before the formation of a thermal oxide layer affects their electrical characteristics. In fact, it is reported that the nature of thermal oxide layers depends on the kind of the chemical oxide layers.<sup>8)</sup>

### §2. Experimental

Phosphorus-doped n-type Si(100) wafers with a resistivity of 10  $\Omega$ cm were washed with boiled acetone and distilled water, and etched in 1% hydrofluoric acid. A thin chemical oxide layer was formed by immersing the wafers in following solutions: i)  $\text{H}_2\text{SO}_4 : \text{H}_2\text{O}_2 = 2 : 1$  at 100  $^\circ\text{C}$  for 10 min, ii)  $\text{HNO}_3$  at 115  $^\circ\text{C}$  for 10 min, and iii)  $\text{HCl} :$

$\text{H}_2\text{SO}_4 : \text{H}_2\text{O} = 1 : 1 : 5$  at 80  $^\circ\text{C}$  for 10 min. The devices formed with solutions i, ii, and iii are hereafter called the  $\text{H}_2\text{SO}_4$  device, the  $\text{HNO}_3$  device, and the  $\text{HCl}$  device, respectively. A  $\sim 3$  nm-thick Pt layer was deposited on the silicon oxide layers by an electron beam evaporation method.

XPS spectra were recorded using an Ulvac-Phi 5500 spectrometer. Monochromatic Al K $\alpha$  radiation was irradiated from the Pt layer side at the incident angle of 45' and photoelectrons were collected in the surface-normal direction, i.e., the take-off angle of 90', unless otherwise mentioned. During the XPS measurements, the front Pt layer was connected to the ground and the bias voltage was applied to the rear Si surface.

### §3. Results and discussion

The substrate Si 2p<sub>3/2</sub> peak shifted toward the lower binding energy upon applying a forward bias, while it shifted in the higher energy direction by applying a reverse bias. These shifts are caused by the charge accumulated in interface states in the Si band-gap. Namely, by applying a forward bias, for example, the Si quasi-Fermi level is elevated, and consequently, the interface states present between the metal Fermi level and the Si quasi-Fermi level are newly occupied by electrons. This negative charge induces a change of the potential drop across the oxide layer, and hence, the substrate Si 2p level at the interface is shifted by the same amount. Therefore, by analyzing the amount of the energy shift of the substrate Si 2p peak measured as a function of the bias voltage,

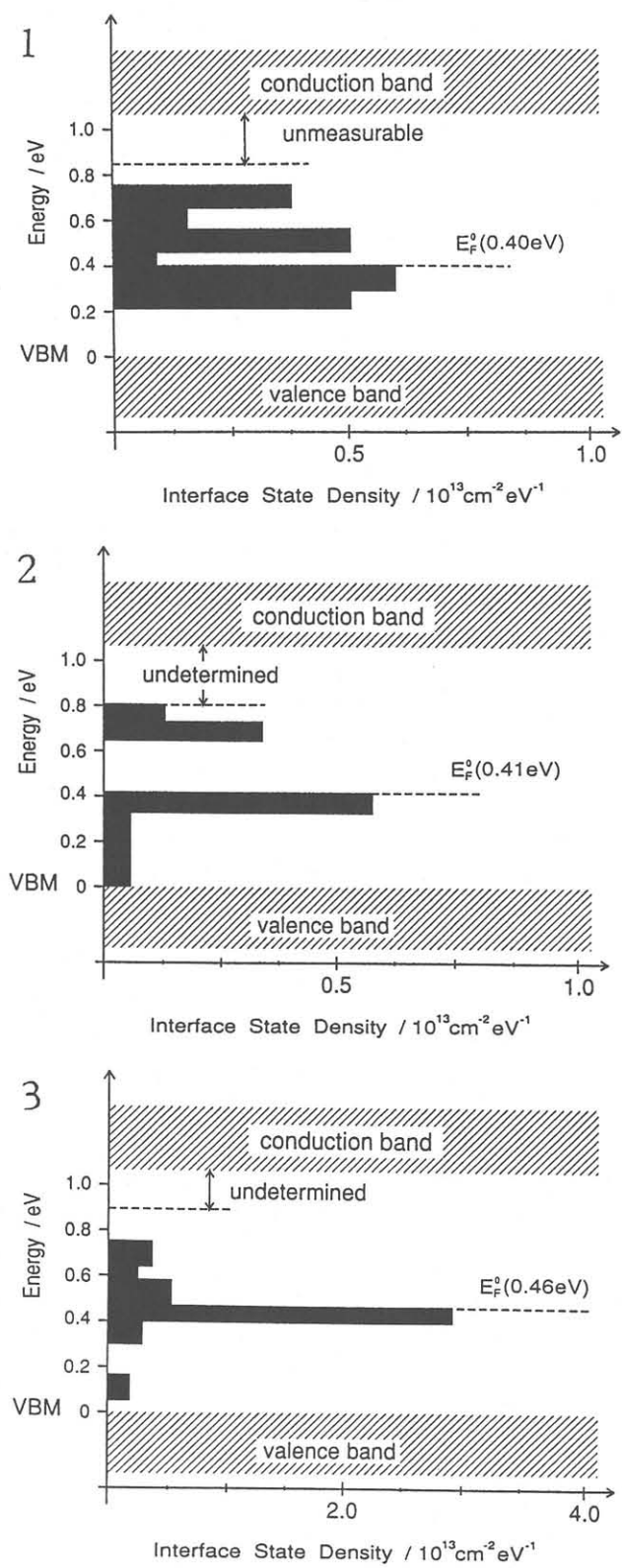


Fig.1. Energy distribution of interface states in the Si band-gap for the (3 nm-Pt/silicon chemical oxide/n-Si(100)) MOS devices with the chemical oxide layers grown in the following solutions: 1)  $H_2SO_4 : H_2O_2 = 2 : 1$  at 100 °C for 10 min, 2)  $HNO_3$  at 115 °C for 10 min, and 3)  $HCl : H_2SO_4 : H_2O = 1 : 1 : 5$  at 80 °C for 10 min.

the energy distribution of the interface states can be obtained.<sup>4-7)</sup>

Figure 1 shows the energy distribution of interface states for the MOS devices. Figs. 1-1, 1-2, and 1-3 are for the  $H_2SO_4$  device, the  $HNO_3$  device, and the  $HCl$  device, respectively. The interface Fermi level,  $E_F^0$ , was obtained from the intercept of the current-voltage curves measured in the dark and under illumination.<sup>6, 7)</sup> The energy distribution for the  $H_2SO_4$  device has three peaks at ~0.3, ~0.5 and ~0.7 eV above the valence band maximum (VBM) with the densities of  $\sim 1 \times 10^{12}$ ,  $\sim 5 \times 10^{11}$ , and  $\sim 4 \times 10^{11} \text{ cm}^{-2}$ , respectively. For the  $HNO_3$  device, on the other hand, two peaks are present at ~0.3 and ~0.7 eV above VBM and the densities of the 0.3 eV- and 0.7 eV-peaks are  $\sim 4 \times 10^{11}$  and  $\sim 5 \times 10^{11} \text{ cm}^{-2}$ , respectively. The  $HCl$  device has only one peak at ~0.5 eV with much higher density of  $\sim 1.4 \times 10^{12} \text{ cm}^{-2}$  than the other devices.

All the observed interface states have discrete energy levels, but do not have U-shaped energy distribution expected from the Coulombic model<sup>9)</sup> and the bond model<sup>10)</sup>. The obtained energy distribution supports the defect model.<sup>11, 12)</sup> Sakurai and Sugano<sup>11)</sup> calculated that the Si dangling bonds interacting weakly with Si and oxygen atoms in the silicon oxide layer have energy levels below and above the midgap, while the isolated Si dangling bonds induce the energy level near the midgap. Therefore, the 0.3 eV-, 0.5 eV-, and 0.7 eV-interface states are attributed most probably to the Si dangling bond interacting with a Si atom, the isolated Si dangling bond, and that interacting weakly with an oxygen atom, respectively.

Table 1 shows the amounts of the various species in the oxide layers estimated from the deconvoluted Si 2p spectra for the chemical oxide-covered Si surfaces with no Pt overlayer. In Table 1-1, the intensities of the oxide species are normalized by that of the substrate peaks, while in Table 1-2, they are normalized by the oxide peaks due to  $Si^{4+}$ . Table 1-1 can be used to see the amount of the species in the oxide layer, while from Table 1-2, we can see where the species are mainly present. For all the specimens, the amount of the  $Si^+$  species, i.e., Si atoms to which one oxygen atom is bound each, is higher in the case of the photoelectron take-off angle of 90° than that for the take-off angle of 20°. This result indicates that the  $Si^+$  species is present mainly near the Si/oxide interface. It is clearly seen that the amount of the  $Si^+$  species in the  $HNO_3$  oxide layer is much

Table 1. Amounts of various species in the silicon oxide layers estimated from the deconvoluted XPS spectra in the Si 2p region.

l-1		H <sub>2</sub> SO <sub>4</sub> device				
take-off angle	Si <sup>+</sup>	Si <sup>2+</sup>	Si <sup>3+</sup>	Si <sup>4+</sup>	Si-H	
90°	0.26	0.07	0.06	1.18	0.36	
		HNO <sub>3</sub> device				
take-off angle	Si <sup>+</sup>	Si <sup>2+</sup>	Si <sup>3+</sup>	Si <sup>4+</sup>	Si-H	
90°	0.12	0.10	0.08	2.59	0.62	
		HCl device				
take-off angle	Si <sup>+</sup>	Si <sup>2+</sup>	Si <sup>3+</sup>	Si <sup>4+</sup>	Si-H	
90°	0.16	0.03	0.06	0.87	0.30	
l-2		H <sub>2</sub> SO <sub>4</sub> device				
take-off angle	Si <sup>+</sup>	Si <sup>2+</sup>	Si <sup>3+</sup>	Si <sup>4+</sup>	Si-H	
90°	2.2	0.6	0.5	10	3.0	
20°	1.5	0.9	1.0	10	1.6	
		HNO <sub>3</sub> device				
take-off angle	Si <sup>+</sup>	Si <sup>2+</sup>	Si <sup>3+</sup>	Si <sup>4+</sup>	Si-H	
90°	0.5	0.4	0.3	10	2.4	
20°	0.3	0.4	0.4	10	1.2	
		HCl device				
take-off angle	Si <sup>+</sup>	Si <sup>2+</sup>	Si <sup>3+</sup>	Si <sup>4+</sup>	Si-H	
90°	1.8	0.3	0.7	10	3.4	
20°	1.3	1.1	0.6	10	2.6	

lower than that in the other oxide layers. It is expected that the interface state density strongly depends on the amount of the Si<sup>+</sup> species because the Si<sup>+</sup> species has structure that, when the Si-O bond is ruptured, it becomes interface states. This expectation is supported by the experimental result that the interface state density for the HNO<sub>3</sub> device is the lowest.

The Si-H species, i.e., Si atoms to which one H atom and three Si atoms are bound each, is present mainly near the Si/oxide interface. The amount of the Si-H species in the HNO<sub>3</sub> oxide layer is higher than that in the other oxide layers (Table 1-1). It is likely that protons in the solution easily

react with the isolated Si dangling bond to form the Si-H species, because free space is present near the isolated Si dangling bonds. This expectation is verified by the result that the HNO<sub>3</sub> device has the highest-density Si-H bonds and the lowest-density isolated Si dangling bond interface states.

The density of the isolated Si dangling bond interface states is the highest for the HCl device. However, the amount of the Si-H species in the HCl oxide layer and that in the H<sub>2</sub>SO<sub>4</sub> oxide layer are almost identical to each other (Table 1-1). It is found by the XPS measurements that in the HCl oxide layer, a considerable amount of Cl is included. Therefore, it is inferred that the high-density interface states for the HCl device are formed by the replacement of bridging oxygen atoms at the interface by Cl<sup>-</sup> ions, resulting in the formation of Si dangling bonds and Si-Cl species.

#### References

- 1) C. N. Berglund, IEEE Trans. Electron Devices ED-13 (1966) 701.
- 2) L. M. Terman, Solid-State Electron. 5 (1962) 285.
- 3) E. H. Nicollian and A. Goetzberger, Bell Syst. Tech. J. 46 (1967) 1055.
- 4) H. Kobayashi, T. Mori, K. Namba, and Y. Nakato, Solid State Commun. 92 (1994) 249.
- 5) H. Kobayashi, Y. Yamashita, T. Mori, Y. Nakato, K. H. Park, and Y. Nishioka, Surf. Sci. 326 (1995) 124.
- 6) H. Kobayashi, Y. Yamashita, T. Mori, Y. Nakato, T. Komeda, and Y. Nishioka, Jpn. J. Appl. Phys. 34 (1995) 959.
- 7) H. Kobayashi, K. Namba, T. Mori, and Y. Nakato, Phys. Rev. B in press.
- 8) G. Gould and E. A. Irene, J. Electrochem. Soc. 134 (1987) 1031.
- 9) A. Goetzberger, V. Heine, and E. H. Nicollian, Appl. Phys. Lett. 12 (1968) 95.
- 10) R. B. Laughlin, J. D. Joannopoulos, and D. J. Chadi, The Physics of SiO<sub>2</sub> and Its Interfaces, ed. S. T. Pantelides (Pergamon, New York, 1978) Chap 6.
- 11) T. Sakurai and T. Sugano, J. Appl. Phys. 52 (1981) 2889.
- 12) A. H. Edwards, Phys. Rev. B 36 (1987) 9638.